

## THEORETICAL STUDY OF THE REACTION RATES OF $\text{OH} + \text{OH} \rightleftharpoons \text{H}_2\text{O} + \text{O}$

LAWRENCE B. HARDING AND ALBERT F. WAGNER

*Theoretical Chemistry Group*

*Chemistry Division, Argonne National Laboratory, Argonne, IL 60439*

The rate constants for the forward and reverse reaction of  $\text{OH} + \text{OH}$  to form  $\text{H}_2\text{O} + \text{O}$  are calculated with variational transition state theory using an *ab initio* MCSCF electronic structure characterization of the reaction path on the two potential energy surfaces that correlate reactants with products. With the scaling of the potential barrier so as to match experiment at room temperature, excellent agreement with experiment for the forward direction is obtained over the full temperature range, including a sharp upward curvature above 1000 K. The excited state surface is shown to be important in this curvature, contributing over 35% of the rate constant at higher temperatures. For the reverse direction, it is argued that the  $\text{H}_2\text{O} + \text{O}$  measured rates are about a factor of two too large, although this difference could be largely accounted for by uncertainty in the equilibrium constant. The calculated rate constants can be represented by the functional forms:

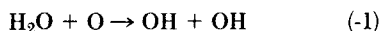
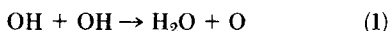
$$k_1(T) = 2.04 \times 10^{-20} T^{2.62} e^{944.9/T} \text{ cm}^3/\text{molec-sec}$$

$$k_{-1}(T) = 2.46 \times 10^{-19} T^{2.60} e^{-7637/T} \text{ cm}^3/\text{molec-sec}$$

over the temperature range of 300 K to 2000 K.

### Introduction

The reaction



are chain-terminating in the forward, or chain-branching in the reverse, direction and therefore influence flame propagation.<sup>1</sup> These two reactions have been critically reviewed by Cohen and Westburg.<sup>2</sup> Ten experimental studies<sup>3-14</sup> of Rxn. (1) are listed in the review. While the measurements are primarily clustered around room temperature, there are two studies<sup>3,4</sup> at high temperatures. These studies indicate strong upward curvature in the rate constant with decreasing inverse temperature. There has been only one experimental study<sup>15</sup> of Rxn. (-1). The measured rate was claimed to be consistent with the forward rate through the equilibrium constant. Results presented here will question that claim.

The consistency of the forward and reverse rates is the first of three issues in contention concerning this reaction. The second concerns the number of different potential energy surfaces that contribute to the reaction rate. Since OH is  $^2\Pi$ , there are four triplet and four singlet surfaces that arise out of

the OH + OH asymptote. Since the products are of triplet spin [ $\text{H}_2\text{O}(^1\text{A}) + \text{O}(^3\text{P})$ ], only the four triplet surfaces could be directly involved in the reaction. Wagner and Zellner<sup>4</sup> discuss the possibility that one of the four singlet surfaces, the one that includes stable hydrogen peroxide,  $\text{HOOH}$ , could be indirectly involved in the reaction through a surface crossing to a triplet surface. They conclude that this is unlikely and thus decide that different reaction routes of different spin multiplicities could not contribute to the overall rate. This analysis still leaves open the possibility of different triplet surfaces with different activation energies being involved in the upward curvature of the rate constant.

The third issue is the importance of long-range forces in controlling the rate. OH has a reasonably strong dipole and quadrupole moment and thus strong electrostatic forces might be sufficiently attractive so as to suppress any barrier on the potential energy surface due to chemical forces. Then only angular momentum barriers on the attractive long-range potential restrict the reactants and control the size of the rate constant. Wagner and Zellner<sup>4</sup> concluded such from an indirect analysis of their measurements. However this analysis is surprising because the strong upward curvature of the rate constant observed by others<sup>3,4</sup> is not usually con-

sistent with a rate constant controlled by angular momentum, rather than potential, barriers.<sup>16</sup>

In this article, the first two issues are directly addressed and the results indirectly relate to the third issue of long-range forces. In Section II, we present *ab initio* calculations of the barrier region on two triplet surfaces. In Section III, the calculated information is used in a variational TST to calculate rates on both surfaces whose sum is compared to experiment. Adjustments in the barrier heights for both surfaces are required. The success of these calculations in reproducing the experimental results argues indirectly that long-range forces are not required by the experiment. Section IV is a discussion section.

### *Ab Initio* Electronic Structure Calculations

In order to calculate the rate constant, the reactants, products, and reaction path must be characterized in terms of structure, frequency, and energetics. This must be done for each triplet surface that connects to the products. There are altogether four triplet surfaces arising from the ground-state reactant asymptote. For planar geometries, two of these surfaces are of  $^3A'$  symmetry and two are of  $^3A''$  symmetry. Only one surface of each symmetry connects ground state reactants with ground state products, so two surfaces must be characterized.

Both surfaces are complicated by the presence of relatively sharp avoided crossings with the other surface of the same symmetry. The cause of these avoided crossings is that while at the transition state the lowest wavefunctions each have singly-occupied radical orbitals on the central oxygen pointing toward the approaching hydrogen, on the reactant side of the transition state, the lowest states each have double-occupied, lone pair orbitals pointing toward this hydrogen (forming a hydrogen bond). Thus there is a sudden change in the character of the lowest wavefunctions as the two OH's approach, from hydrogen bonding at larger distances to radical abstraction near the transition states.

Two levels of electronic structure calculations are used, multi-configuration self-consistent field, MCSCF, and singles and doubles configuration interaction, GVB + 1 + 2, calculations.<sup>17</sup> Both sets of calculations employ a polarized double zeta basis set. The MCSCF calculations are used to locate and characterize the transition state structures. The configurations included in the MCSCF calculations are as follows: Each OH bond is correlated with two orbitals. All three possible occupations of two electrons in each of the two orbitals are included. Both sets of oxygen lone pair electrons are treated by allowing full CI's of 5 electrons in 3 orbitals.

The four sets of configurations thus defined are multiplied together to give the final set of 100 MCSCF configurations.

The MCSCF calculations were carried out on both the  $^3A'$  and  $^3A''$  surfaces at a sufficient number of points to define a planar anharmonic force field in the vicinity of the two transition states. Convergence problems, due to the mixing of the two states, made it impossible to determine out-of-plane force constants. For this reason the out-of-plane force constant was chosen such that the out-of-plane frequency at the transition state matched that for the OH + H<sub>2</sub> reaction.<sup>18</sup> Reaction path analyses were then carried out using these force fields. As noted above, sharp avoided crossings are found on the reactant side of the transition state. These crossings cause problems both in the convergence of the MCSCF calculations and in the fitting of the force field. For this reason it was not possible to follow the reaction path very far on the reactant side of the transition state.

The geometries of the two transition states obtained from the MCSCF calculations are shown in Fig. 1. The calculated MCSCF barriers are 18.2 and 19.6 kcal/mole for the  $^3A'$  and  $^3A''$  states respectively. Although the above calculations are expected to lead to a qualitatively accurate description of the transition state region, the barriers calculated with these wavefunctions are much too high due to the neglect of a large fraction of the correlation energy.

In order to ascertain the affect of the neglected correlations on the locations and the energy separation of the two transition states, a limited number of GVB + 1 + 2 calculations were also carried out. These calculations include over 150,000 configurations and thereby account for a much larger fraction of the total correlation energy. The GVB + 1 + 2 calculations were carried out along the MCSCF reaction path in order to determine whether or not

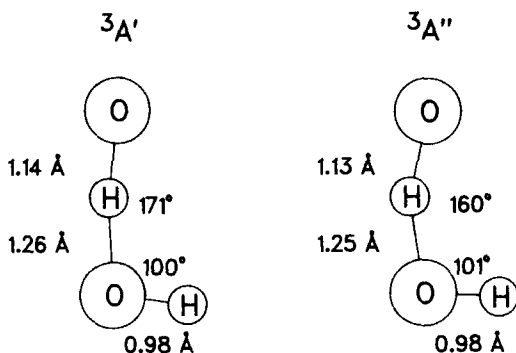


FIG. 1. MCSCF structures for the  $^3A'$  and  $^3A''$  transition states.

the added correlations shift the locations of the two barriers. The GVB + 1 + 2 barriers, obtained in this manner, are 7.7 and 10.1 kcal/mole for the  $^3\text{A}''$  and  $^3\text{A}'$  states respectively. Plots of both the MCSCF and GVB + 1 + 2 energies along the reaction path are shown in Figure 2. From this plot it can be seen that the GVB + 1 + 2 calculations do not significantly shift the locations of either barrier relative to the MCSCF results. Note that the GVB + 1 + 2 barriers are also expected to be too large.

The major conclusions from the electronic structure calculations then are that two low-lying transition states for this reaction exist. The two transition states are very similar in structure but separated by approximately 2.4 kcal/mole in energy.

The two extended curves in Fig. 2 are the optimized scaling of the calculated potential energy curves so as to maximize agreement at room temperature with experiment (as will be discussed in the next section). The GVB + 1 + 2 barriers are too large to be consistent with experiment because of the relatively small basis set used here. Errors of  $\sim 5$  kcal/mole in calculated barrier heights, as indicated in the figure, are not unusually large for a polarized double zeta basis set.

Figure 2 also shows a negative region of the potential on the reactant side of the transition state that represents hydrogen bonding. The structure, frequency, and energetics of the hydrogen-bonded configuration on the two surfaces are assumed to be essentially identical to that determined from GVB + 1 + 2 calculations on the analogous singlet surfaces for  $\text{OH} + \text{OH}$ .<sup>19</sup> The placement of the hy-

drogen-bonded configuration along the reaction coordinate,  $s$ , in Fig. 2 is based on the assumption that, starting from the saddle point, motion along  $s$  toward reactants proceeds in two stages. First, the reacting H moves to its equilibrium distance with the reactant O. The directly calculated portion of the reaction path confirms this approximation for H movement two thirds of the way to the equilibrium position. The remaining one third distance must be assumed. Second, the two O—H molecules separate, without orientation change, to the calculated O—O distance of the hydrogen-bonded configuration. This is likely as the saddle point and hydrogen-bonded structures are calculated to have similar orientations. With this two stage assumption, a value for  $s$  of  $-1.95 a_0$  can be assigned to the hydrogen-bonded configuration. A continuous potential curve is produced by exponential functions that match in slope and value the directly calculated portions of the path. While the hydrogen-bonded portion of the curve has no direct influence on the rate constants, had it not been included, variational effects could have altered the calculated rate constants (see Section IV).

Experimental Morse parameters<sup>20</sup> were used to describe the OH reactants. The  $\text{H}_2\text{O}$  product was described by the Schatz-Elgersma potential energy surface<sup>21</sup> which reproduces to beyond the harmonic level the experimental force field. The reaction exoergicity was adjusted slightly (by 0.2 kcal/mole) so as to make the calculated equilibrium constant agree with the JANAF value<sup>20</sup> which includes anharmonic effects and rotational-electronic coupling (in OH) ignored here. Over the temperature range of 300 K to 2000 K, the JANAF equilibrium constant was reproduced to within 2%.

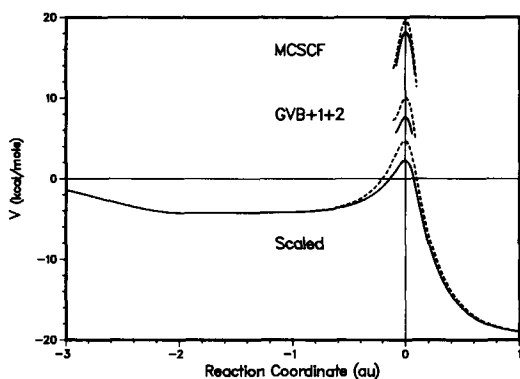


FIG. 2. MCSCF, GVB + 1 + 2 and scaled potential energy curves along the reaction coordinate. The reactants,  $\text{OH} + \text{OH}$ , are at a reaction coordinate of  $-\infty$  and the products,  $\text{H}_2\text{O} + \text{O}$  are at  $+\infty$ . The solid and dashed curves refer to the  $^3\text{A}''$  and  $^3\text{A}'$  states, respectively.

### Rate Constant Calculations

Given the above characterization of the reactants, products, and the reaction path in the vicinity of the barrier to reaction, the rate constant in either direction can be calculated with improved variational transition state (ICVT) theory<sup>22</sup> corrected for tunneling with a small curvature semiclassical adiabatic ground state (SCSAG) transmission coefficient. ICVT/SCSAG rate constants have proven reliable<sup>22,23</sup> by comparison to experiment or to other more rigorous calculations. There are limitations to the application of this method to  $\text{OH} + \text{OH}$  which are discussed in the next section. The program POLYRATE<sup>24</sup> was used to carry out the calculations.

As discussed previously, the directly calculated barrier height on either surface is too large and must be scaled. The scaling criteria was to match the

theoretical rate constant with the consensus experimental one for Rxn. (1) at room temperature. The 2.4 kcal/mole difference between the barrier heights on the two surfaces was preserved in the scaling because the MCSCF and GVB + 1 + 2 values for this separation are about the same even though the values for the reaction barrier differ by about a factor of two (see Fig. 2). The resulting rate constant as a function of inverse temperature is plotted for Rxn. (1) in Fig. 3 and for Rxn. (-1) in Fig. 4. The final scaled barriers have already been presented in Fig. 2.

The calculated results in Fig. 3 show excellent agreement with experiment. In particular, the sharp upward curvature of the rate constant at temperatures above 1000 K is confirmed. As the figure indicates, the rate constant on the excited  $^3A'$  surface is important in that upward curvature, contributing about 35% of the total rate constant at 2000 K but only about 10% at room temperature. The relatively flat low-temperature behavior is due to the fact that the dominant  $^3A''$  rate constant experiences the near cancellation of two conflicting influences with increasing temperature: the decrease in tunneling and the increase in surmounting the reaction barrier. The calculated rate constant from 300

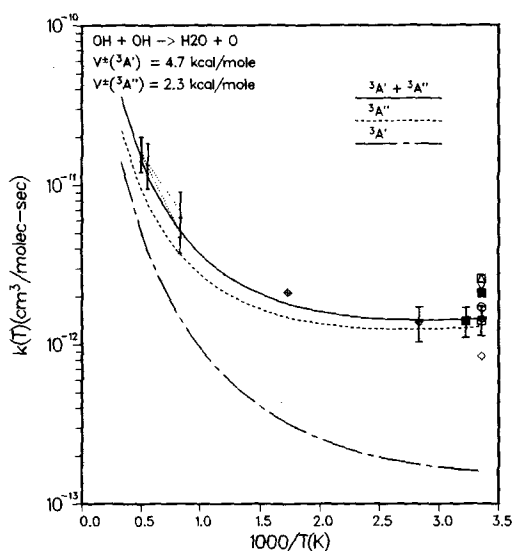


FIG. 3. Comparison of theoretical rate constants for  $\text{OH} + \text{OH} \rightarrow \text{H}_2\text{O} + \text{O}$  with experimental results:  $\diamond$ , Ref. 5;  $\blacksquare$ , Ref. 6;  $\square$ , Ref. 7;  $\triangle$ , Ref. 8;  $\diamond$ , Ref. 9;  $\nabla$ , Ref. 10;  $\bullet$ , Ref. 11;  $\square$ , Ref. 12;  $\boxtimes$ , Ref. 13;  $\circ$ , Ref. 14;  $\cdots$ , Ref. 3 (lower curve) and Ref. 4 (higher curve).  $V^\ddagger$  is the final optimized barrier height (without zero-point correction) for the listed surface.

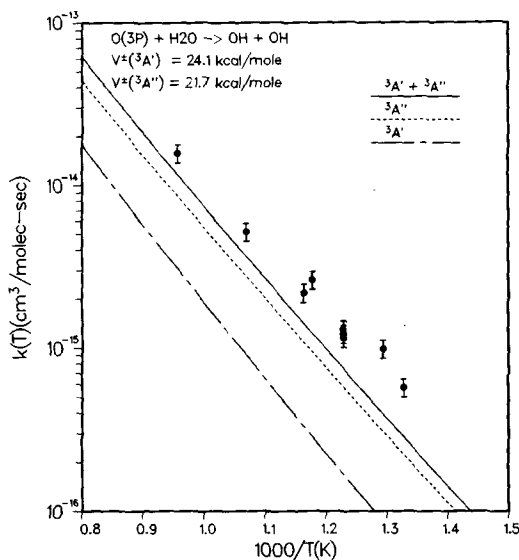


FIG. 4. Comparison of theoretical rate constants for  $\text{H}_2\text{O} + \text{O}$  with experimental results of Ref. 15.  $V^\ddagger$  is the final optimized barrier height (without zero-point correction) for the listed surface.

K to 2000 K agrees to within 3% with the expression:

$$k_1(T) \approx 2.04 \times 10^{-20} T^{2.62} e^{944.9/T} \text{ cm}^3/\text{molec-sec} \quad (2)$$

Note that in this fitted form, the strong upward curvature of the rate constant is primarily carried by the high power of  $T$ .

In Fig. 4, the agreement of the final calculated rate constant for the reverse Rxn. (-1) with the single experimental measurement is poor, generally underestimating the experimental rate constant by a factor of two. As mentioned above, the exoergicity used in the calculation was slightly adjusted so that the calculated equilibrium constant closely reproduces the experimental value. The difference in Fig. 4 is well beyond the small residual errors between the calculated and experimental equilibrium constant. This indicates either an inconsistency in the experimental measurements in the forward and reverse directions or an error in the equilibrium constant.

Since there are no measurements of Rxn. (1) over the same temperature range (750 K–1050 K) as Rxn. (-1) in Fig. 4, a direct analysis of any inconsistency is not possible. However, if the reaction barrier is scaled to reproduce the measurements of Rxn. (-1), then the calculations can be used to predict the rate

constant of Rxn. (1) at room temperature where there are many measurements. This scaling reduces the barrier on both surfaces by about 1.0 kcal/mole which results in a room temperature rate constant for Rxn. (1) about 2.3 times larger than the calculated value in Fig. 3 and above all of the low temperature measured values. This suggests the measured values of  $\text{H}_2\text{O} + \text{O}$  are the ones in error, being too high by about a factor of two. If this is the case the theoretical rate constant in Fig. 4 represents the best available estimate of the rate constant  $\text{H}_2\text{O} + \text{O}$ . That rate constant agrees from 300 K to 2000 K to within 4% with the expression:

$$k_{-1}(T) = 2.46 \times 10^{-19} T^{2.60} e^{-7637/T} \text{ cm}^3/\text{mole-sec} \quad (3)$$

An alternative explanation is that the equilibrium constant is in error. A reduction in the OH heat of formation by the limit of its uncertainty (0.3 kcal/mole<sup>30</sup>) would so change the equilibrium constant as to remove most of the difference between theory and experiment in Fig. 4. Since the heat of formation of  $\text{H}_2\text{O}$  and O are very well known and since two OH molecules constitute one of the asymptotes, the equilibrium constant for Rxns. (1) and (-1) are exceptionally sensitive to the OH heat of formation. Only further experiments can clarify if the measured  $\text{H}_2\text{O} + \text{O}$  rate constant or the OH heat of formation is in error.

### Discussion

The calculations presented above have three approximations that are difficult to evaluate. First, the scaling of the potential is severe (a 75% reduction from the GVB + 1 + 2 values) and is presumed to occur with no alteration in the frequency or structure along the reaction path. Only electronic structure calculations too large to be currently feasible can test this approximation. Second, the extrapolated portion of the reaction path to the hydrogen bonding configuration can only be regarded as qualitative. No portion of the extrapolated path contributes to the calculated rate constant and in that sense there is no approximation. However, this extrapolation does eliminate any strong variational effects normally expected of a heavy-light-heavy mass combination.<sup>23,25</sup>

Variational effects occur because the zero point energy locked into motion perpendicular to the reaction path drops more rapidly than the potential energy increases as the saddle point is approached. In heavy-light-heavy systems, a high light-heavy reactant frequency (here a  $3800 \text{ cm}^{-1}$  OH stretch)

changes to a small heavy-heavy symmetric stretch saddle point frequency (here a  $400 \text{ cm}^{-1}$   $\text{O}\cdots\text{H}\cdots\text{OH}$  stretch) suggesting a strong drop in zero point energy. However, the results for Rxns. (1) and (-1) show that variational effects never change the rate constant by more than about 10% from that calculated by conventional transition state theory.

Over the narrow range of  $s$  values where the *ab initio* calculations could be carried out (see Fig. 2), no frequencies changed significantly and thus the directly calculated portion of the path is free of strong variational features. However, in the extrapolated portion of the path, some frequency change must occur to make up the more than one kcal/mole change in zero point energy from reactants to saddle point. In this region the potential is dropping to the stabilized hydrogen-bonding energy of about -4.3 kcal/mole. That drop of the potential eliminates any variational effects along the extrapolated portion of the reaction path, even given the fact that the zero point energy at the hydrogen-bonding configuration is almost three kcal/mole higher than that at the saddle point. If the extrapolated portion of the curve were to qualitatively change, such variational effects could become important and influence the rate constant.

The last approximation concerns the small curvature approximation (SCSAG) used in the tunneling. Heavy-light-heavy systems have relatively large curvature of the reaction path allowing tunneling to "cut the corner" of the potential energy ridge separating the reactant and product troughs on the potential energy surface. SCSAG does not incorporate this mechanism and may therefore underestimate the tunneling. The importance of this effect for any system higher than triatomic has never been determined and its calculation would be beyond the scope of this work. In triatomic studies,<sup>25</sup> large curvature corrections have been important only when variational effects are important, which is not the case here.

Because of the qualifications just mentioned, the results presented in this article can not be regarded as conclusive. Nonetheless, they suggest answers to the three questions posed in the introduction. First, the calculations support an inconsistency in the  $\text{OH} + \text{OH}$  and  $\text{H}_2\text{O} + \text{O}$  measurements and suggest the latter measurements are too high by a factor of two. (An alternative explanation is that the OH heat of formation is too high by 0.3 kcal/mole.) Second, some of the non-Arrhenius curvature of the rate constant at high temperatures is due to two different routes to reaction, with each route having the same spin multiplicity of triplet. The two triplet surfaces are estimated to be about 2.4 kcal/mole different from each other at the transition state. Third, the excellent agreement between experiment and theory for Rxn. (1) indicates a long-range

electrostatic model is not required by the measured results. A barrier to reaction of about 2.3 kcal/mole is indicated.

### Acknowledgment

The authors thank Dr. R. Steckler for assistance with the POLYRATE program. This work performed under the auspices of the Office of Basic Energy Sciences, Division of Chemical Sciences, U.S. Department of Energy, under Contract W-31-109-Eng-38.

### REFERENCES

1. WARNATZ, J.: *Combustion Chemistry* (W. C. Gardiner, Jr., Ed.) p. 197, Springer-Verlag, 1984.
2. COHEN, N. AND WESTBURG, K. R.: *J. Phys. Chem. Ref. Data*, 12, 531 (1983).
3. RAWLINS, W. T. AND GARDINER, JR., W. C.: *J. Chem. Phys.*, 60, 4676 (1974).
4. ERNST, J., WAGNER, H. GG. AND ZELLNER, R.: *Ber. Bunsenges. Phys. Chem.*, 81, 1270 (1977).
5. WAGNER, G. AND ZELLNER, R.: *Ber. Bunsenges. Phys. Chem.*, 85, 1122 (1981).
6. DEL GRECO, F. P. AND KAUFMAN, F.: *Disc. Faraday Soc.*, 33, 128 (1962); KAUFMAN, F.: *Ann. Geophys.*, 20, 106 (1964).
7. DIXON-LEWIS, G., WILSON, W. E. AND WESTENBERG, A. A.: *J. Chem. Phys.*, 44, 2877 (1966).
8. WILSON, W. E. AND O'DONOVAN, J. T.: *J. Chem. Phys.*, 47, 5455 (1967).
9. BREEN, J. E. AND GLASS, G. P.: *J. Chem. Phys.*, 52, 1082 (1970).
10. WESTENBERG, A. A. AND DEHAAS, N.: *J. Chem. Phys.*, 58, 4066 (1973).
11. MCKENZIE, A., MULCAHY, M. F. R. AND STEVEN, J. P.: *J. Chem. Phys.*, 59, 3244 (1973).
12. CLYNE, M. A. A. AND DOWN, S.: *J. Chem. Soc. Faraday Trans. II*, 70, 253 (1974).
13. TRAINOR, D. W. AND VON ROSENBERG, JR., C. W.: *J. Chem. Phys.*, 61, 1010 (1974).
14. FARQUHARSON, G. K. AND SMITH, R. H.: *Aust. J. Chem.*, 33, 1425 (1980).
15. ALBERS, E. A., HOYERMAN, K., WAGNER, H. GG. AND WOLFRUM, J.: *Thirteenth Symposium (International) on Combustion*, p. 81, The Combustion Institute, 1971.
16. CLARY, D. C.: *Molec. Phys.*, 53, 3 (1984).
17. DUNNING, T. H. JR., AND HARDING, L. B.: *Theory of Chemical Reaction Dynamics* (M. Baer, Ed.), Vol. 1, p. 1, CRC Press, 1985.
18. SCHATZ, G. C., WALCH, S. P.: *J. Chem. Phys.*, 72, 776 (1980).
19. HARDING, L. B., unpublished results.
20. CHASE, JR., M. W., CURNUTT, J. L., DOWNEY, JR., J. R., McDONALD, R. A., SYVERUS, A. N., VALENZUELA, E. A.: *J. Phys. Chem. Ref. Data*, 11, 695 (1982); JANAF Thermochemical Tables, 1982 Supplement, and references therein.
21. SCHATZ, G. C. AND ELGERSMA, H.: *Chem. Phys. Lett.* 73, 21 (1980).
22. TRUHLAR, D. G., ISAACSON, A. D., GARRETT, B. C.: *Theory of Chemical Reaction Dynamics* (M. Baer, Ed.), Vol. 4, p. 65, CRC Press, 1985.
23. TRUHLAR, D. G., HASE, W. L. AND HYNES, J. T.: *J. Phys. Chem.*, 87, 2264 (1983).
24. ISAACSON, A. D., TRUHLAR, D. G., RAI, S. N., STECKLER, R., HANCOCK, G. C., GARRETT, B. C., AND REDMON, M. J.: *Computer Physics Communications*, 47, 91 (1987).
25. BONDI, D. K., CONNOR, J. N. L., GARRETT, B. C. AND TRUHLAR, D. G.: *J. Chem. Phys.* 78, 5981 (1983).

### COMMENTS

J. A. Miller, *Sandia National Laboratories, USA*. Is the lack of temperature dependence you observe at low T simply the effect of tunneling cancelling the "classical" effect of the energy barrier?

Does your small-curvature tunneling approximation increase or decrease the effect of tunneling that one would predict from a one-dimensional calculation?

*Author's Reply.* The lack of a temperature dependence at low T is primarily due to the effect you mention, i.e., the cancelling of the activation energy from the classical barrier by quantum mechanical tunneling through the barrier. In regards to the small curvature approximation, it only slightly

increased the tunneling over over a one-dimensional calculation without this approximation.

•

G. Nyman, *Univ. of Göteborg, Sweden*. You showed results from a rate constant calculation using Clary's adiabatic capture model. The rate constant you obtained was much too large as a result of the assumption in the adiabatic capture model that all reactants approaching each other closer than the position of the centrifugal barrier will react. Would it be feasible, and if so, sensible, to do the adiabatic capture model calculation with the criterion for reaction being that the highest barrier in

the effective potential should be passed and not only the outer, purely centrifugal barrier?

*Author's Reply.* In this study, we indicate that the true bottleneck to reaction is at a chemical barrier about 2–3 kcal/mole high at a close distance of approach between the two hydroxyl radicals. As mentioned in the talk but not in the above paper, if an adiabatic capture theory is applied to the known long-range dipole-dipole forces for  $\text{OH} + \text{OH}$ , the rate constant is seriously overestimated. If adiabatic capture theory were applied, as you suggest, over both the chemical and electrostatic part of the potential energy surface, then the theory should also locate the reaction bottleneck in the vicinity of the chemical barrier. However, the quantitative accuracy of the rate constant calculated by such a theory depends on the specific nature of the adiabatic capture theory. Generally, such theories do not include tunnelling, implicitly retain the rotational quantum number of the reactants in the description of the reaction bottleneck, and in some applications (i.e., an infinite order sudden version as was used in our calculations) favor a sudden over an adiabatic description of the reaction. In our rate constant calculations reported in this paper, a variational transition state theory is used which does include tunnelling, uses a bending degree of freedom description of the reaction bottleneck, and adopts

an adiabatic description of the reaction process. Such transition state calculations in the past have been very successful in describing reactions with chemical barriers and would be expected to be more accurate than a "typical" adiabatic capture rate constant calculation extended to chemical barriers.

•

*J. Wolfrum, Univ. of Heidelberg, Fed. Rep. of Germany.* How are the different fine structure states of the  $\text{O}(^3\text{P})$  atom taken into account for the  $\text{O}(^3\text{P}) + \text{H}_2\text{O}$  reaction?

*Author's Reply.* The fine-structure states of  $\text{O}(^3\text{P})$  were handled in an adiabatic way. Thus the rate constant without any fine-structure considerations is multiplied by the ratio of the electronic partition function at the transition state and at the reactants. The electronic partition function at the transition state is set to three for the triplet state under the approximation that the fine-structure splitting for the transition state is essentially zero. The fine structure of the OH in the OH + OH direction of the reaction is handled in exactly the same way. Thus the equilibrium constant in the calculation correctly includes the fine-structure effects at each asymptote.